University of New Mexico
UNM Digital Repository

2-14-2014

High Temperature Polymer Dielectrics For Electric Vehicle Capacitor Applications

Kylen Johns

Follow this and additional works at: https://digitalrepository.unm.edu/cbe_etds

Recommended Citation

Kylen Johns
Candidate

Chemical and Nuclear Engineering
Department

This thesis is approved, and it is acceptable in quality and form for publication:

Approved by the Thesis Committee:

Plamen Atanassov, Chairperson

Cy H. Fujimoto

Dimiter N. Petsev

**HIGH TEMPERATURE POLYMER DIELECTRICS FOR
ELECTRIC VEHICLE CAPACITOR APPLICATIONS**

by

KYLEN SHANEL JOHNS

B.S., Chemical Engineering, University of New Mexico, 2012

THESIS

Submitted in Partial Fulfillment of the
Requirements for the Degree of

Master of Science

Chemical Engineering

The University of New Mexico
Albuquerque, New Mexico

December 2013

ACKNOWLEDGEMENTS

Corporation, for the U.S. Department of Energy's National Nuclear Security Administration under contract DE-AC04-94AL85000.

HIGH TEMPERATURE POLYMER DIELECTRICS FOR ELECTRIC VEHICLE CAPACITOR APPLICATIONS

By

Kylen Shanel Johns

B.S., Chemical Engineering
Master of Science, Chemical Engineering

ABSTRACT

Currently there is a push for low cost, high energy materials with high operating temperatures that can simultaneously reduce cost, weight, and volume in the automotive industry. Economically feasible high performance capacitors are critical to the Department of Energy's goal to advance technologies that will ensure energy security and reduce the use of petroleum while reducing cost and environmental impacts. [1] Recent studies have been done to improve the inverter systems in hybrid electric vehicles (HEVs). HEVs require inverters to convert direct current to alternating current which prevents damage to the battery and powers the electric motor. Current thin film DC bus capacitors are the least reliable component of HEV inverters and require 30% of the total inverter volume. They also represent up to 23% of the inverter cost and weight and have a maximum operation temperature of no greater than 105 °C. [2, 3] In order to reduce cost and volume of these inverters there is a significant need for the development of high temperature dielectric materials for use in HEVs. The overall goal of this project was to develop inexpensive, high energy density, high temperature polymer-based dielectrics and capacitors to replace current DC bus capacitors.

TABLE OF CONTENTS

Chapter 1

Introduction

Three projects were funded under the APEEM portfolio by the Vehicle Technologies (VT) Office through the Power Electronics and Electric Motors department which focused on decreasing high temperature capacitor cost, weight, and volume. The three projects focused on thin PLZT films on foil capacitors, thin glass capacitors, and polymer-based dielectrics such as ours. Ceramics such as silicon oxide, silicon nitride, and barium titanate have been investigated for use in power capacitors, but the dielectric loss is large and the processing of materials can be complicated and expensive. [4] Venkat *et al.* reports that polymer dielectrics are the material of choice for applications such as power capacitors because of their low dissipation factors, high breakdown strengths, and good dielectric stability over a range of temperatures and frequencies despite their inherently lower dielectric constants compared to ceramic capacitors. [5] In addition, they are capable of large scale processing into films at a relatively lower cost. An added benefit of polymer film capacitors is the properties that facilitate a graceful failure mechanism, or a gradual loss in capacitance rather than a catastrophic failure often witnessed in ceramic capacitors. Due to this fact, polymer dielectric capacitors can be operated at electric fields closer to the breakdown strength allowing higher energy densities. [3]

Much research has been done in the subject of dielectric polymer films for power applications in recent years. [5-7] The current state of the art polymer films are made from biaxially oriented polypropylene (BOPP) due to a low dissipation factor (DF) and

high breakdown voltage strength. This material has a maximum operating temperature of 105 °C and is seldom used in environments above 85 °C. [7]   Nash reports that polypropylene became the choice in power capacitors due to its low cost as well as its ability to be processed, a critical criterion for the manufacturability of power capacitors due to the required high winding speed in the winding of capacitor rolls. [8]   Other materials have been investigated including polyester (PE) and polycarbonate (PC). Anderson *et al.* shows that PE has a maximum operating temperature of 125 °C but tends toward a higher dissipation factor with increasing frequency and temperature giving it limited use in power electronic applications. [6] PC also has an operating temperature of 125 °C and can provide low DF but has reliability issues and is the most expensive of the three aforementioned.   Some other commercially available polymer film capacitors include poly(ethylene terephthalate) (PET), poly(ethylene napthalate) (PEN), poly(phenylene sulfide) (PPS), and Teflon ®. Only PPS and Teflon ® can be operated above 150 °C; however, Teflon ® demonstrates low breakdown strengths, and PPS has poor self-healing capabilities in addition to being expensive. [3, 6] Consequently, none of these options satisfy the VT program's requirements for reliability and temperature of capacitors.

Winsor *et al.* reports that polyvinylidene fluoride (PVDF) has been given some attention in the last two decades due to the material's intrinsic high dielectric constant but exhibits many problems including poor clearing (self-healing) abilities and higher dissipation factors as well as relatively lower breakdown voltages and poor mechanical properties. [9] Others have reported similar studies of fluid impregnated film capacitors;

however, these capacitors have a very slim range of operating temperatures, often less than 100 °C except for those of PPS and polyimides. [8, 9]

Chapter 2

Materials and Methods

Polymer Film Capacitor Preparation

General Preparation of Solvent Cast Polymer Films

Polymers excluding TOPAS® were dissolved into $CHCl_3$ overnight and cast into thin films (20-30 µm) on a Teflon substrate using a Gardco automatic drawdown machine. TOPAS® was dissolved in xylenes and heated to 80 °C. Upon solvent evaporation at room temperature the film was removed from the substrate and placed in a vacuum oven for 12 hours at 65 °C to remove any residual solvent. The film was then metallized with a solid layer of 50 nm Au on one side of the free standing film and 6.3 mm diameter electrodes of the same thickness on the opposite side using a Cressington 108 sputter coater in preparation for electrical characterization. Thicknesses were measured using a Dectak profilometer.

Electrical Evaluation Procedure

A Hewlett Packard 4284A Precision LCR meter was used to measure the capacitance for the small test capacitors at 10 kHz and 5 kV. The dielectric constant of the polymer films were measured and the DC breakdown field was found using a Trek 30/20A with an amplified voltage ramp at 500 V/s. The probability of failure was calculated based on the thickness and area of the polymer dielectric. Breakdown measurements were taken with metallized polymer films on a Cu plate submerged in Fluorinert® FC-40 purchased from Sigma Aldrich.

Thermal Characterization

A TA Instruments Q200 and Q500 were used for differential scanning calorimetry (DSC) and thermogravimetric analysis (TGA) respectively. DSC was used to determine the glass transition temperature of the polymers by measuring how much the heat capacity (Cp) is changed by temperature. A sample of known mass was heated in an aluminum pan, and the changes in heat capacity were measured as changes in heat flow. The DSC was run from 20 °C to 250 °C under nitrogen and repeated for three cycles. An RCS 90 cooling unit was used to bring down the temperature of the cycle. TGA was used to characterize decomposition behavior of the polymers by measuring weight changes in the material as a function of temperature. Samples of known mass were heated from room temperature to 800 °C at a rate of 10 °C per minute in a platinum pan under nitrogen.

Mechanical Characterization

A TA Instruments Q800 DMA was used to measure the stress versus strain of the polymer films with a film/fiber tension clamp fixture. The measurements were made with a ramp force of 3 N/min to 18 N/min.

Prototype Capacitor Preparation

Stacked capacitor films were cut into 5 by 4 inch rectangles and double stacked on layers of 5 by 3 inch discrete Al (6 μm thick) foil sheets. Rolled capacitor films were cut into 10 by 3 inch rectangular strips and stacked on layers of 9 by 3 inch discrete Al (6 μm thick) foil sheets. Al leads were attached to each of the foil layers for measurement purposes. Both forms of capacitors were then hot pressed at ~190 °C.

Chronoamperometry Measurements

A Gamry Reference 600 Potentiostat/Galvanostat/ZRA was used for chonoamperometry measurements. 2-NDPA was incorporated into 9.7% (w/w) S-POW in chloroform solutions in concentrations discussed in Chapter 2. A glassy carbon electrode with a surface area of 0.03 cm^2 was polished and sonicated in EtOH for 15 minutes prior to each measurement. 5 µL of additive solution was dropped onto the electrode and allowed to air dry. The electrode was placed in a 0.1M KOH with 0.1M KCl electrolyte solutions of pH 9.5 and 11.5. A potential was applied starting from -1.0 to1.0 V vs. an Ag/AgCl reference electrode and a Pt wire counter electrode with a step of 0.1 V.

PhNDI Polymer Preparation

Materials

Aniline, carbic anhydride and norbornene were purchased from Acros. Benzaldehyde and Grubb's I and III were purchased from Sigma Aldrich and acetic acid was purchased from Fisher Scientific. Chemicals were used as received. Chloroform was purchased from Acros and bubbled with argon gas overnight.

Monomer Preparation

All monomer synthesis procedures were performed in an argon or nitrogen atmosphere. Details of procedures are included.

150 g of 1:1 *exo:endo* carbic anhydride was heated to 185 °C in a roundbottom flask while using a mechanical stirrer under an argon blanket. Reaction was carried out for 3 hours and then cooled to 85 °C. 150 mL of ethyl acetate was added to the flask and heated to 185 °C. Reaction was then allowed to cool to room temperature. The white precipitate was filtered and dried to give 150 g. The *exo* product was recrystallized 3 times with ~150 mL ethyl acetate and dried in a vacuum oven at 70 °C overnight to give 39.1 g of 24:1 *exo:endo* carbic anhydride product. 33.9 g of *exo* carbic anhydride was stirred in 255 mL of acetic acid and 19.2 mL of aniline under dry nitrogen. Reaction was refluxed for 4 hours and allowed to cool to room temperature. Pink precipitate was filtered and dried. The product was recrystallized once with toluene and dried in a vacuum oven at 70 °C overnight to give 45.5 g.

Polymerization Procedure for (*exo*-PhNDI)

All (*exo*-PhNDI) polymerizations were carried out under argon at room temperature in chloroform that was degassed overnight. Reactions were terminated using 0.10 mL benzaldehyde, and polymer was precipitated into ethanol. Acquired polymer was filtered and dissolved in ~250 mL dichloromethane and re-precipitated into ethanol to force *exo* product and purify. 9.5 g of a (40 mmol) was stirred in 150 mL of degassed chloroform until fully in solution. 5.6 mg (0.0066 mmol) of catalyst was then dissolved in 2 mL of chloroform and added to the system. Reaction was terminated after 15 min upon the addition of benzaldehyde.

Copolymerization Procedure for 90 (*exo*-PhNDI) and NBE

9.5 g (40 mmol) of (*exo*-PhNDI) and 0.42 g (4.4 mmol) of norbornene (NBE) were stirred in 150 mL of degassed chloroform until fully dissolved. 5.8 mg (0.0068

mmol) of catalyst was then dissolved in 2 mL chloroform and added to the system. Reaction was terminated after 20 min upon the addition of benzaldehyde.

Copolymerization Procedure for 50 (*exo*-PhNDI) and NBE

The same procedure was followed as the 90 (*exo*-PhNDI) but was performed using 9.5 g (40 mmol) of (*exo*-PhNDI) and 3.7 g (39.3 mmol) of NBE with 6.2 mg (0.0073 mmol) of catalyst.

Copolymerization Procedure for 30 (*exo*-PhNDI) and NBE

The same procedure was followed as the 90 (*exo*-PhNDI) but was performed using 9.5 g (40 mmol) of (*exo*-PhNDI) and 8.7 g (92.4 mmol) of NBE with 6.1 g (0.0072 mmol) of catalyst.

Chapter 3

Evaluation and Characterization of Additives Incorporated in S-POW

In order for a polymer to be a suitable dielectric for the purpose of HEV applications it must exhibit a relatively high dielectric constant, low dissipation factor, and high breakdown strength. However, breakdown strength has a much greater impact on overall energy density. Future Department of Energy (DOE) VT objectives require inverter operation of 150 °C and 450 V at a volume of 0.6 L. Current polymer-based capacitors also have maximum operating temperatures ranging from 105 °C to 120 °C. [10]

You *et al.* discussed the relation of dielectric constant of a polymer to the degree of polarization; the dielectric constant is larger in molecules with stronger polarity, especially when the polar groups are placed as side chains instead of the backbone of the polymer. [4] Therefore, in order to synthesize molecules with higher intrinsic dielectric constants, functional groups with large dipole moments including cyano, nitro, halogen, perfluoroalkyl groups can be introduced as side chains. Polynorbornenes (PNBEs) are usually considered low dielectric materials due to their symmetric structures; however, the addition of polar side groups was investigated.

In order to achieve the future DOE goals, a high temperature polymer dielectric was developed using ring opening metathesis polymerization (ROMP) with Grubbs 1 ruthenium catalyst. The dielectric is a norbornene (NBE) based material with similar chemical functionality of Kapton® including imide, ether, and aromatic groups. TOPAS® Advanced Polymers currently produces NBE in quantities of 21,000 tons per

year, significantly lowering the cost of the material. The copolymer of poly(NBE) and N-phenyl-7-oxanorbornene (poly(PhONDI)) was synthesized with multiple ratios of monomer PhONDI (n) to NBE (m) as shown in Table 1.

Table 1. Stoichiometry of co-poly(PhONDI)-poly(NBE).

% ONDI (n)	% NBE (m)
0	100
25	75
50	50
75	25

The poly(PhONDI) homopolymer was synthesized but thin films of the material were extremely difficult to work with and too brittle to perform characterization. The 75:25 copolymer was chosen based on relative permittivity, glass transition temperature, and mechanical properties. When polymer solutions were left out in air over 48 hours (in a solvent such as dichloromethane or chloroform) polymer was precipitating out and did not go back into solution when stirring or upon heating. This outcome was determined to be consistent with crosslinking of the double bonds in the backbone of the copolymer which led to the removal of the double bonds, eliminating free radical induced crosslinking.

PNBE based polymers are very prone to oxidative degradation due to the highly unsaturated nature of the polymers. [11] Hydrogenating the olefin in the polymer backbone was the method chosen to increase polymer solution lifetimes and improve the processability of the polymer. Tosylhydrazide was heated, upon which the hydrazide undergoes decomposition, giving the reactive species initiating the hydrogenation. [12] However, more cost effective hydrogenation processes could be used for scale up of the

polymer system including hydrogen gas with a catalyst. Scheme 1 shows the unsaturated copolymer and the resulting copolymer (S-POW) after hydrogenation of the olefins. Details of the synthesis of S-POW can be found in Denton *et al*. [13, 14]
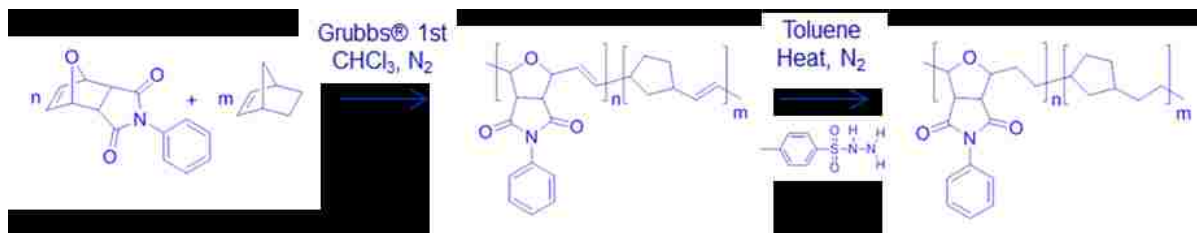
Scheme 1. Synthesis of S-POW (Hydrogenated co-poly(PhONDI)-poly(NBE)).

The dielectric constant of S-POW was found to be 3.08 with a breakdown strength of 350 V/μm and an energy density of 1.62 J/cm^3. The Tg of the material was measured at ~175 °C safely allowing temperature stability of greater than 150 °C. Initially the dielectric was solvent cast into thin films and the capacitors were fabricated using a stacked process. A series of prototype capacitors were developed using a drawdown-based solvent casting technique with a layering of the S-POW films (~20 μm thick) and thin films of aluminum foil (~6 μm). Capacitors (~0.5 μF) were fabricated in-house using the layering technique. Two layers of polymer dielectric were used to minimize the possibility of film defect causing a short.

The packaged capacitors (Figure 1) have a scaled volume of 9.6 liters (based on initial packaging results) for a 1000 μF capacitor; far smaller than the 21.6 liters of current high temperature capacitors. More recent work has demonstrated the use of a rolled form to produce high temperature capacitors with reduced volume (reduced by five

times) relative to the stacked capacitors (based on initial packaging results). The volume reduction in the rolled capacitors is readily apparent in a comparison of each of the prototype forms, each with a similar capacitance of ~1 µF as shown in Figure 2. While the initial volumes of the capacitors fabricated using the Sandia developed polymer are a great improvement in cost, volume, and weight relative to commercially available dielectric materials, they do not meet the VT volume goal.

**Figure 1**. Stacked prototype capacitor with marker for scale.

Figure 2. Stacked vs. rolled prototype capacitor volume comparison with dime for scale.

It has also become apparent from initial attempts to package the capacitors that high temperature packaging materials need to be developed to pot or encase the high temperature dielectric material (Figure 3). A typical epoxy encasing material is liquid prior to curing, and after curing the epoxy is transformed to a solid. The cross-linked epoxy materials typically have glass transition temperatures of ~105-120 °C which means that significant softening can occur at 150 °C. A mitigation strategy would be the inclusion of reinforcing nanoparticles which should increase the Tg of the potting material as this work progresses.

Figure 3. Stacked capacitor potted in epoxy with marker for scale.

Hunt *et al.* discusses a series of certain chemicals that act as voltage stabilizers and offer protection from the effect of small defects in insulation materials such as polyethylene. [15] Therefore, four additives were chosen from this series of organic chemicals and examined in an attempt to increase the breakdown strength of the S-POW by acting as protection from these imperfections. In order to create a baseline for the experiments, an inexpensive commercially available polymer was identified with similar characteristics to S-POW to be used for the additive measurements. This commercially available NBE-based polymer (TOPAS® COC) is a cyclic olefin copolymer that has been used in a variety of applications including high temperature packaging, optical, electronics, and healthcare (Scheme 2). [16]
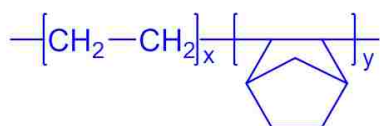
Scheme 2. TOPAS® COC structure.

14

The polymer has a similar price point to BOPP ($8/lb compared to $10/lb for BOPP) and to our knowledge has not been used as a thin film polymer dielectric for capacitor applications. Prior to the additive studies, very thin films of the polymer were fabricated and the electrical properties characterized as a function of temperature. The polymer has good dielectric properties up to 150 °C due to a glass transition temperature of ~175 °C.

A technique different from that of the prototype capacitors was employed to develop capacitors using one thin polymer film (~20 µm) for the purpose of characterization. The films were solvent cast in the same manner discussed previously and metalized using a sputter coating technique with a solid (50 nm thick) gold coating on one side of the film and 30 small electrodes (6.3 mm diameter) of the same thickness on the opposite side. Dielectric permittivity and breakdown testing were performed to determine the effect of 2- and 4-nitrodiphenylamine (NDPA), 4-nitrophenol and 2-nitroaniline. Additive amounts of 0.1, 0.2, 0.5, 1.0 and 5.0% were added to 10% (w/w) TOPAS® solutions and films were then solvent cast and metallized as described previously. The breakdown results were analyzed using Weibull statistics where the cumulative probability of failure follows Equation 1 [17]:

$$P = 1 - e^{\left(\frac{E}{E_0}\right)^{\beta}}$$

Equation 1. CDF used for breakdown evaluation. E_0 is a scale parameter which represents the probability of failure at 62.3%.

Figures 4-7 demonstrate the cumulative distribution functions of each of the chosen additives in the polymer solutions. Structures of the additives are also provided.

Unanticipated difficulties were encountered when attempting to produce TOPAS® films using the drawdown method. A series of solubility tests were performed to determine solvents for casting and the polymer was only soluble in xylenes when heated (80 °C). This created problems with casting due to the low boiling point of xylenes (~140 °C) by causing the formation of pits and overall poor quality of films and potentially contributing to unusual behavior where more of a logarithmic curve is observed in some samples as displayed in Figures 5-7. Based on this analysis, 2-NDPA yielded the most reproducible results and was then incorporated into S-POW in the same concentrations.
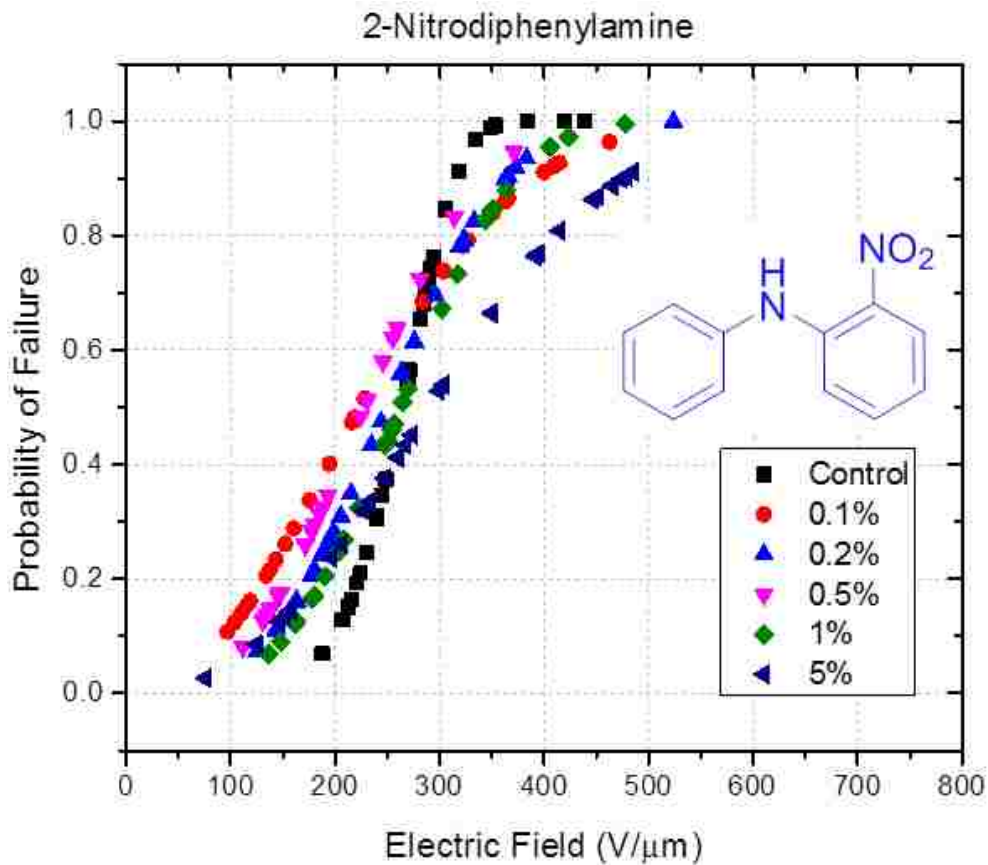

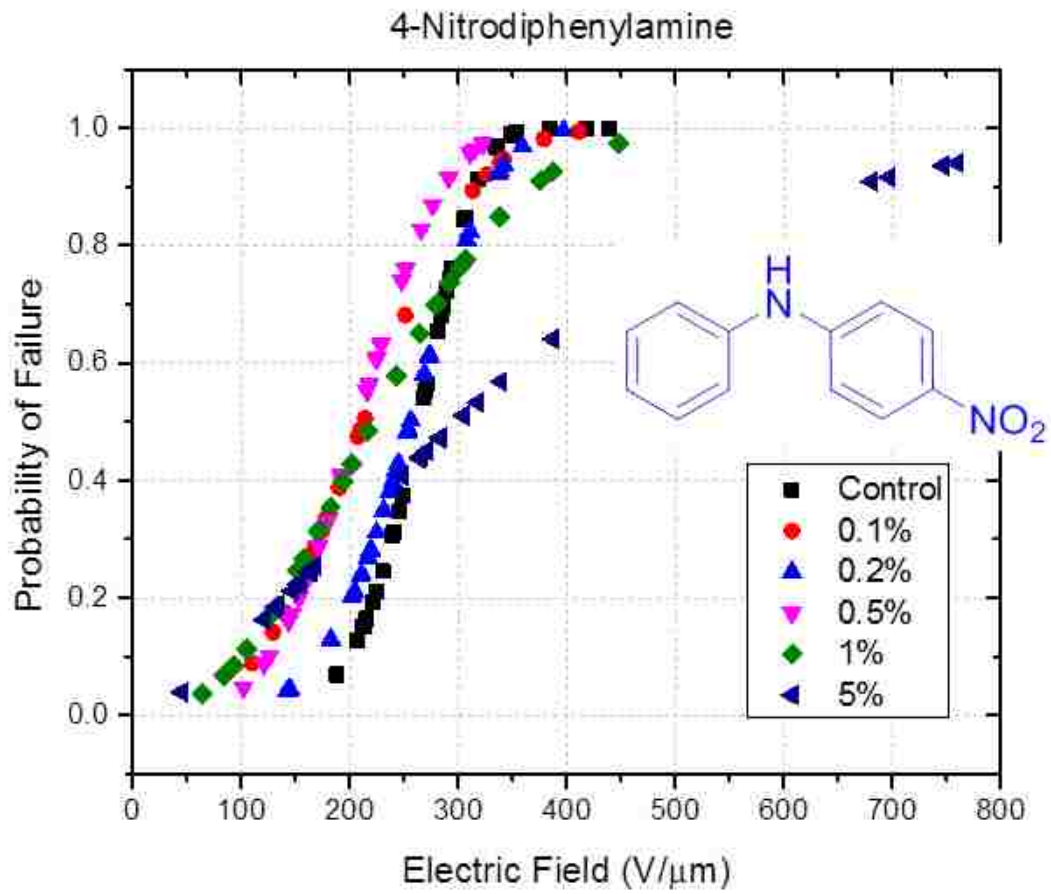**Figure 4.** Breakdown results for 2-NDPA in TOPAS®.

Figure 5. Breakdown results for 4-NDPA in TOPAS®.
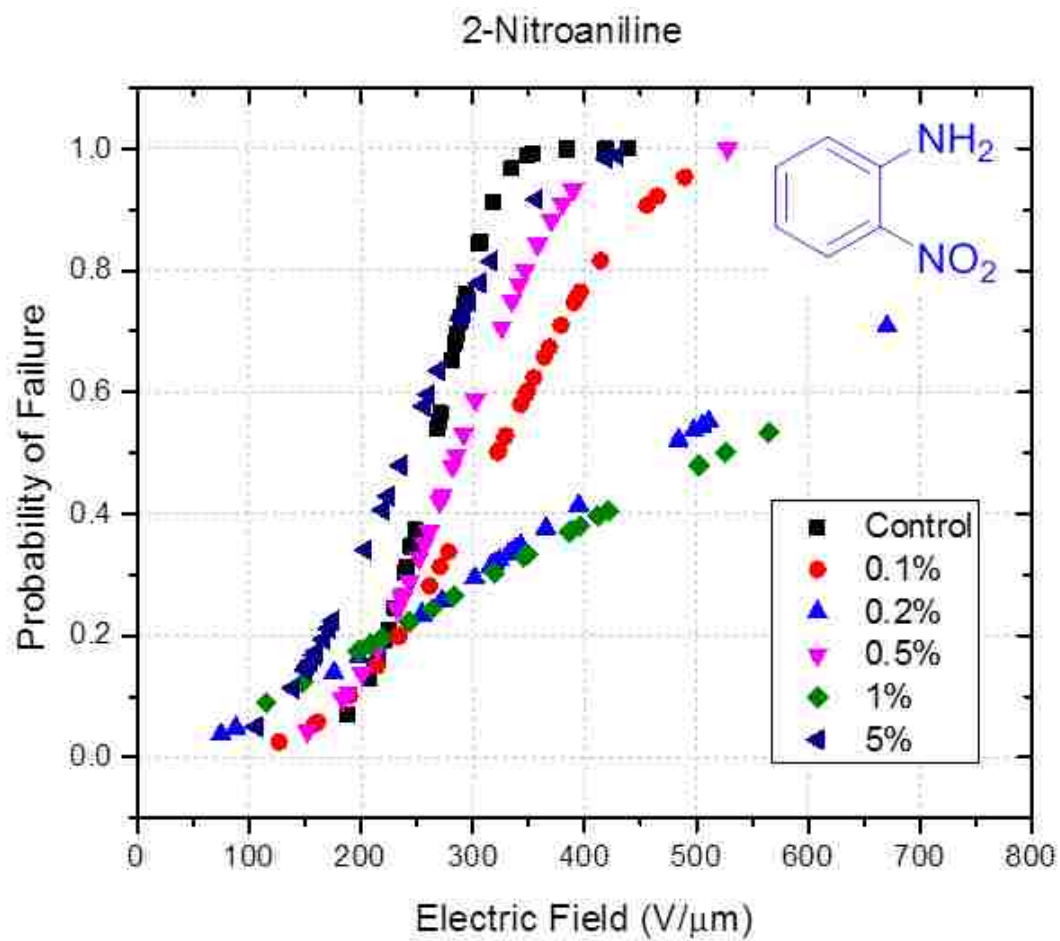
Figure 6. Breakdown results for 2-nitroaniline in TOPAS®.
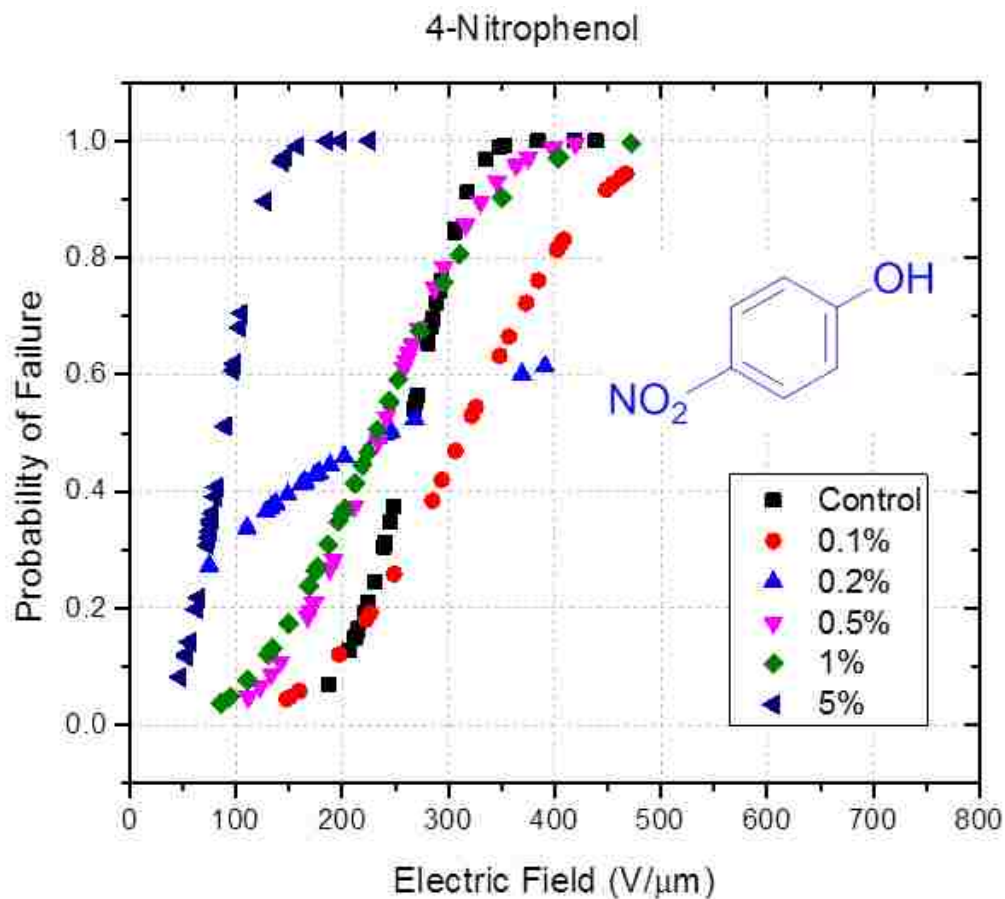
Figure 7. Breakdown results for 4-nitrophenol in TOPAS®.

The incorporation of 2-NDPA showed an increase in breakdown strength (Figure 8) of greater than 50 V/µm at 0.2% and 1.0% (w/w) and an increase of ~25 V/µm at 0.5% from the control S-POW film without a significant increase in dielectric constant or dissipation factor (Figure 9) but an increase in energy density in the three aforementioned (Table 2).
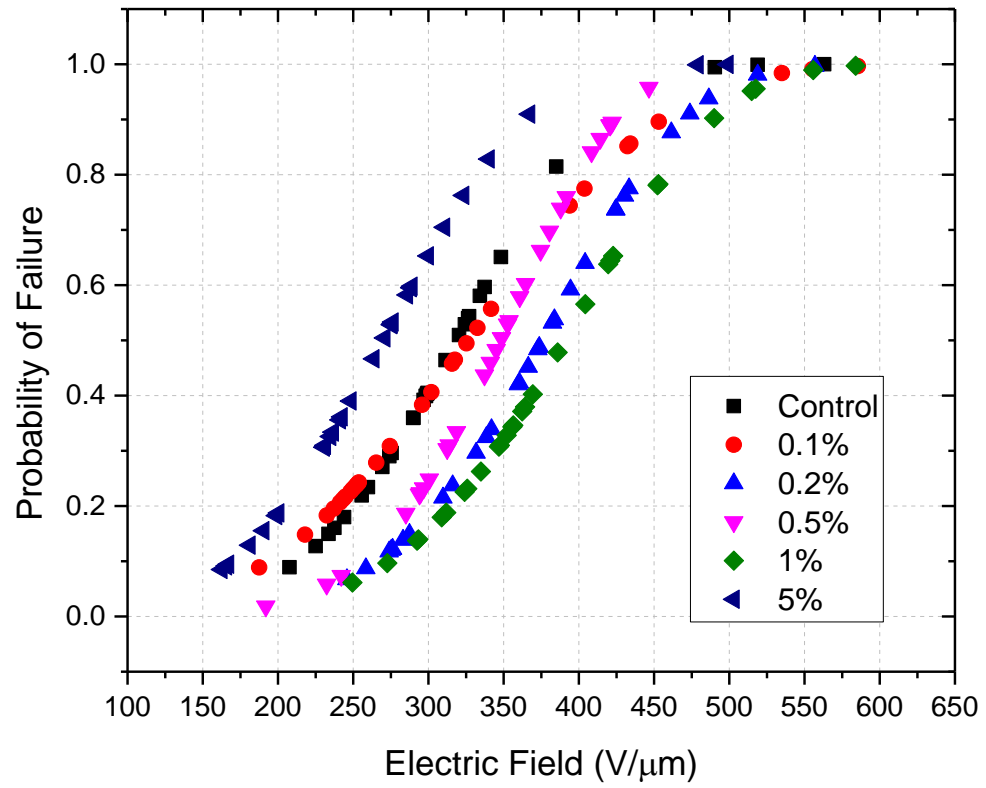
Figure 8. Breakdown results for solvent cast 2-NDPA in S-POW additive/polymer thin film.
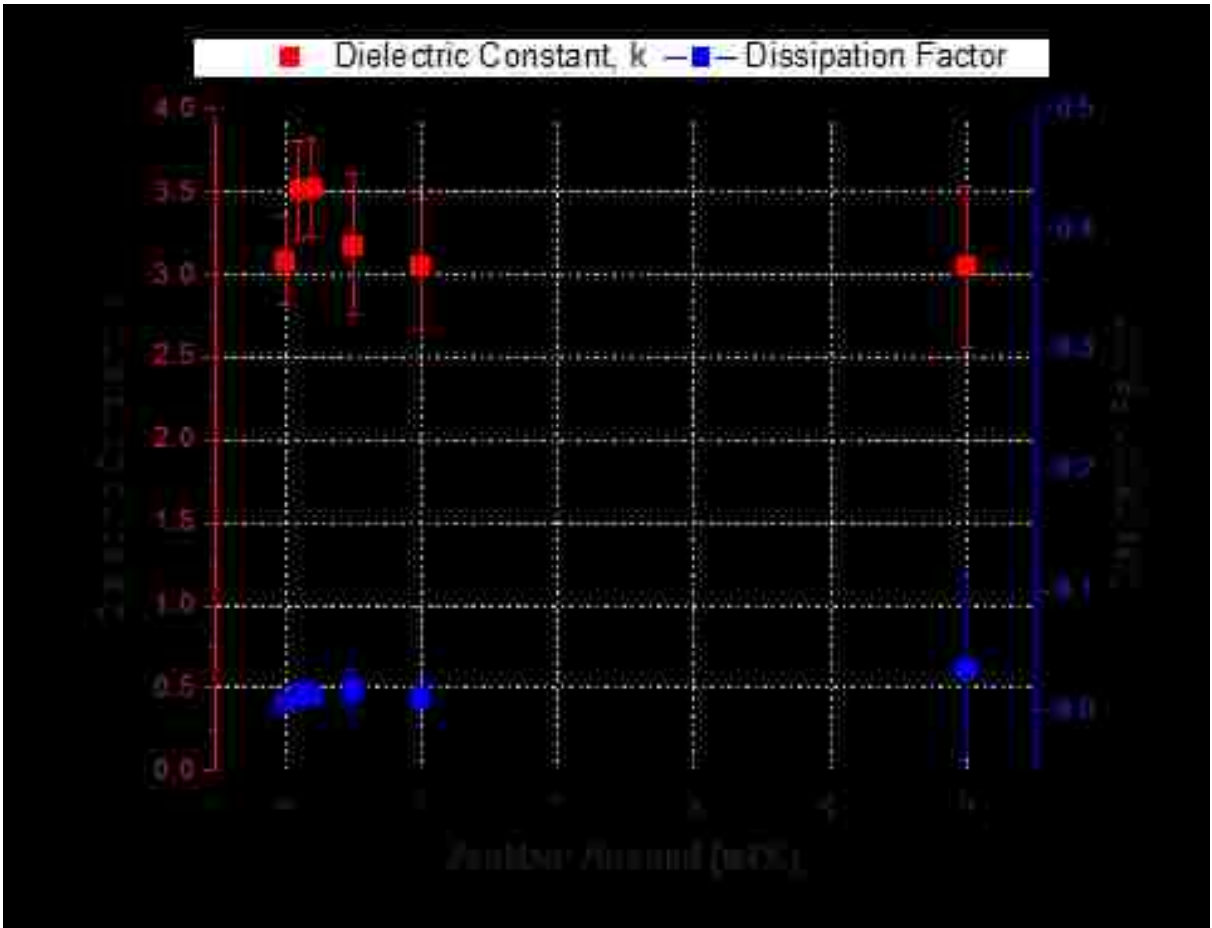
Figure 9. Dielectric constant and DF of additive/polymer film measured at 10 kHz.

Energy density was calculated using Equation 2 where ε_r is the dielectric constant of the material, ε_0 is vacuum permittivity (8.85 pF/m) and V is breakdown (voltage) strength. A graphical comparison of calculated energy densities can be found in Figure 10.

$$U_e = \frac{1}{2}(\varepsilon_r \varepsilon_0 V^2)$$

Equation 2. Energy density equation.

21

Table 2. Measured breakdown strength and calculated energy density of additive/polymer film.

2-NDPA Concentration (w/w)	Breakdown (V/µm)	Energy Density (J/cm³)
0	345	1.62
0.1	365	1.36
0.2	405	2.53
0.5	370	1.76
1.0	415	2.37
5.0	290	1.18
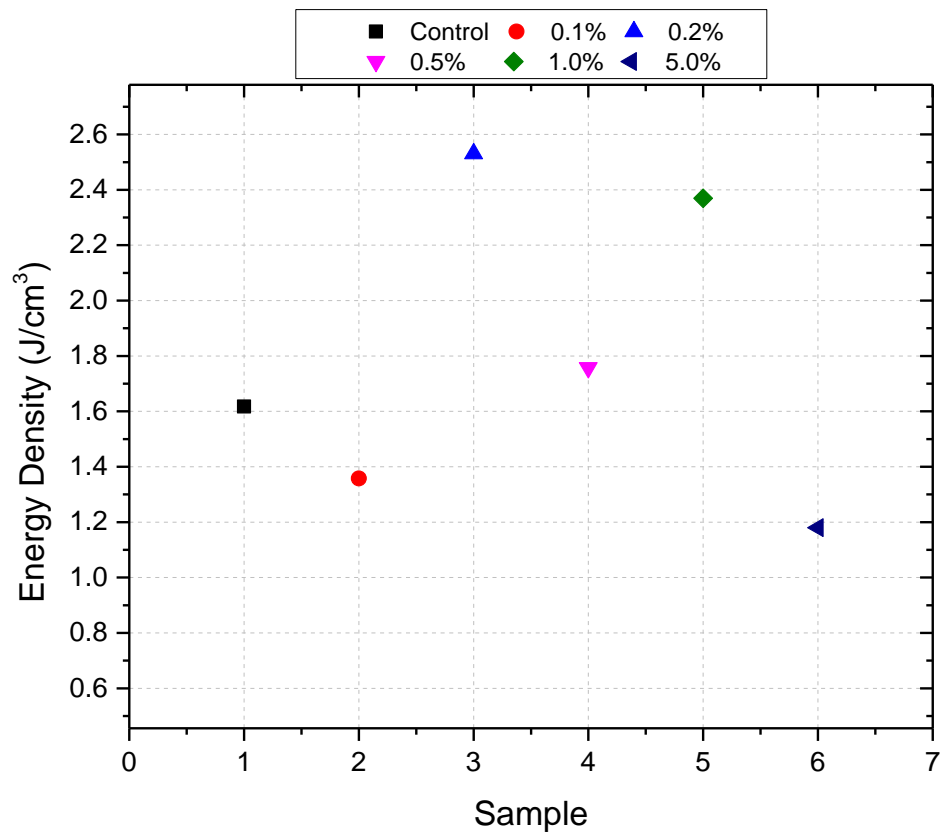
Figure 10. Calculated energy densities of 2-NDPA in S-POW thin films.

The 0.2% and 1.0% (w/w) compositions were compared to S-POW control films using various thermal and mechanical characterization techniques. Differential scanning calorimetry (DSC) and thermogravimetric analysis (TGA) were performed to determine the effect of the additive on T_g and decomposition temperature (T_d) respectively. 2-NDPA was not found to have any significant deteriorating effect on either value as clearly shown in Figures 11 and 12.
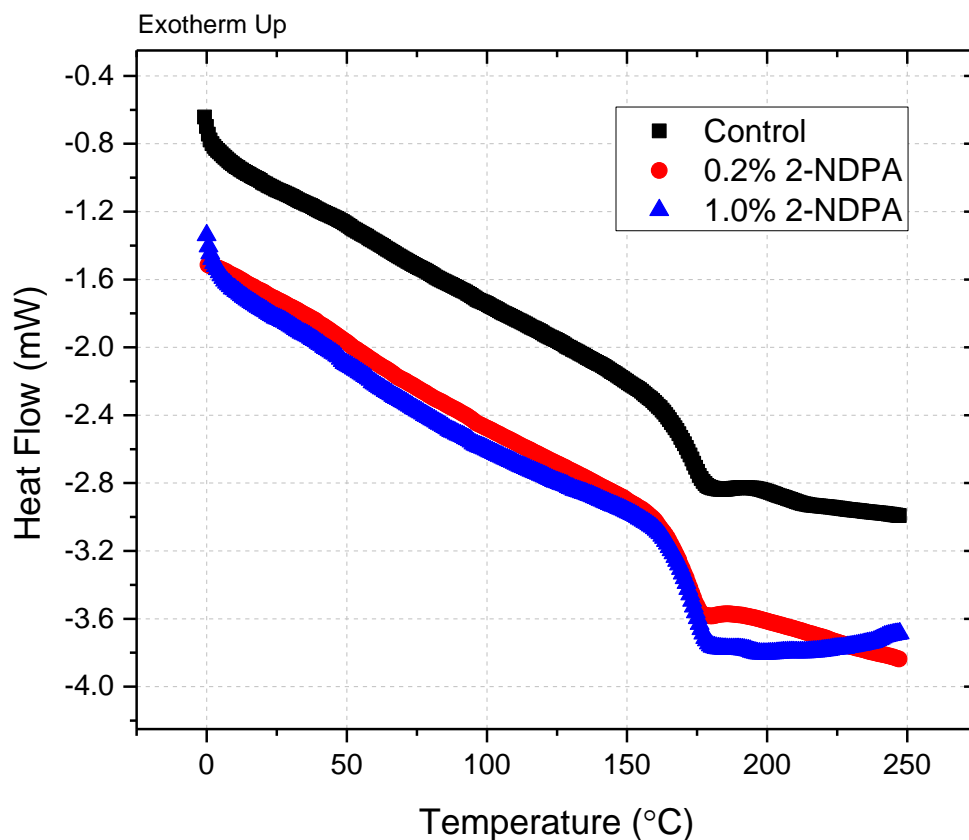
Figure 11. DSC generated comparison of T_g for 1.0% and 0.2% (w/w) additive to S-POW control.
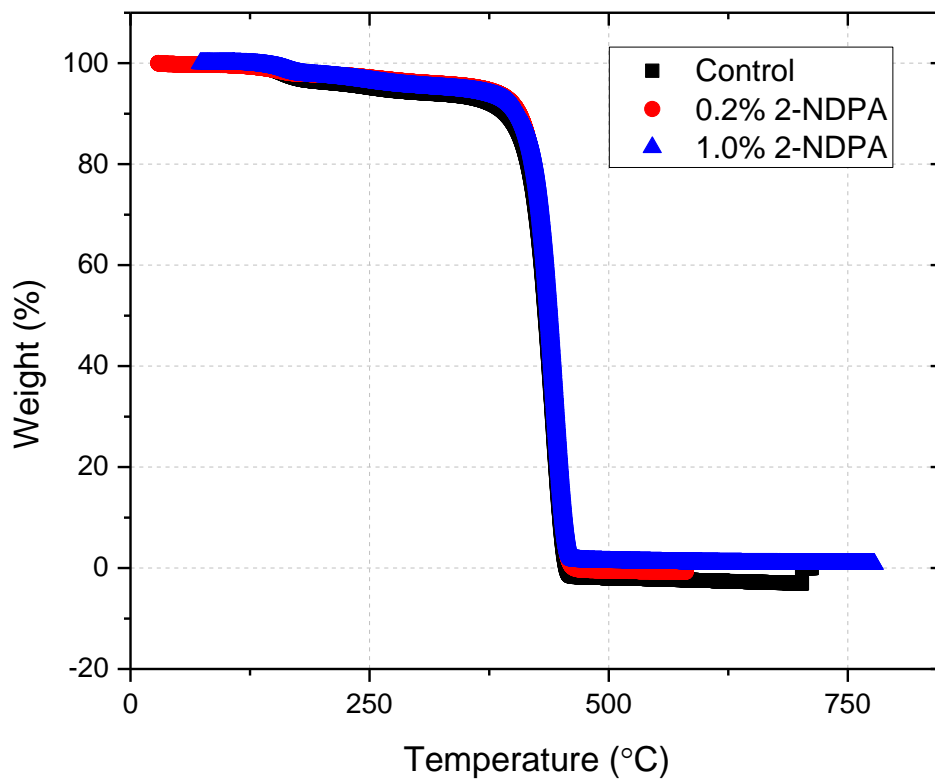
Figure 12. TGA generated comparison of T_d for 1.0% and 0.2% (w/w) additive to S-POW control.

Characterization was performed to investigate the effect of 2-NDPA in S-POW on the films' mechanical properties. A stress-strain curve was developed using dynamic mechanical analysis (DMA) for the S-POW additive films as found in Figure 13. Slight improvements in modulus were observed with additive and no negative consequences were observed.
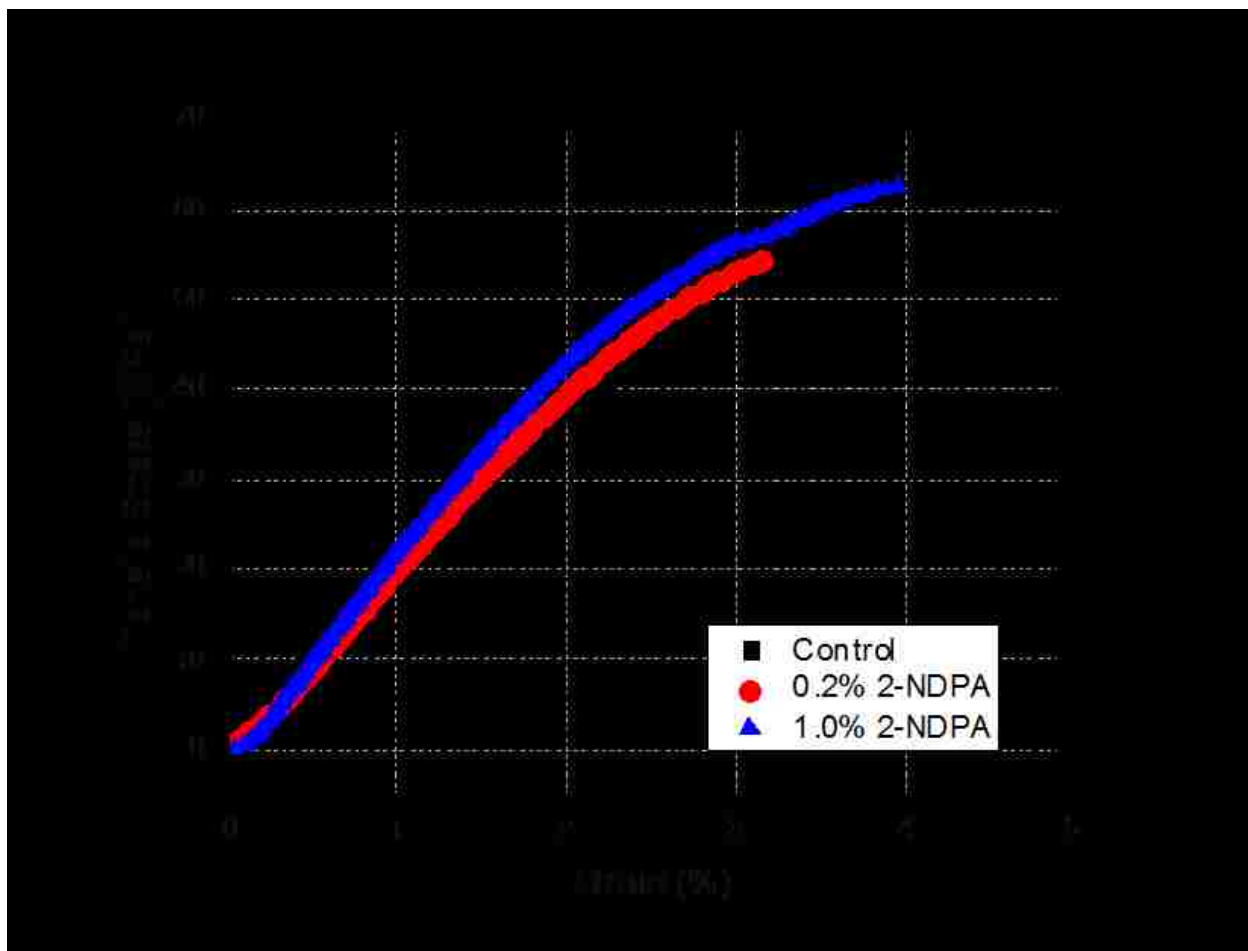
Figure 13. Stress/strain curve comparison for 1.0% and 0.2% (w/w) additive to S-POW control.

The incorporation of 2-NDPA generated significant improvements in the dielectric properties of S-POW by increasing the breakdown strength of the material and leading to an increase in energy density. Electrochemical processes were then examined to develop an understanding of the voltage stabilizing effect of the additive 2-nitrodiphenylamine in S-POW as discussed in Chapter 4.

Chapter 4

Electrochemical Study of Polymer/Additive Composites

In electrochemically active polymers, also named redox polymers or oxidation-reduction polymers, electrons can be transported by an electron exchange reaction (also known as electron hopping). These polymers have spatially and electrostatically localized redox sites that can be ideally reversibly oxidized or reduced. Redox polymers can be separated into different subclasses depending on their chemical structure. Some redox polymers contain covalently attached redox sites that can be located in the backbone of the polymer or as side chains. These oxidation or reduction centers are usually organic or organometallic molecules that can undergo fast electrochemical transformation. There are also ion (proton) exchange polymeric systems known as polyelectrolytes where the active ions are held by electrostatic interactions. Simultaneous electron and ion transfer is also typical for electrochemical insertion reactions.

The exchange current, or current at equilibrium, is the current observed in absence of net electrolysis and at zero overpotential. At equilibrium, potential electron transfer processes at the electrode/solution interface in both directions are carried out, where the forward and reverse reaction rates are equal. This ongoing current in both directions normalized to the electrode surface area is known as exchange current density. At equilibrium conditions, the electrode is known to adopt a potential based on the bulk concentrations of oxidized and reduced species as dictated by the Nernst equation (Equation 3).

$$E_{eq} = E^{0`} + \frac{RT}{nF} \ln \frac{C_O}{C_R}$$

Equation 3: Nernst equation.

Where $E_{eq.}$ is the electrode potential at equilibrium, $E^{0`}$ is the formal redox potential of the reduction reaction, R is the universal gas constant, T is the temperature in Kelvin, n is the number of electrons, F is the Faraday constant and C_O and C_R are the bulk concentration of the oxidized and reduced species.

According to the Butler-Volmer equation (Equation 4) the exchange current, i_0, is proportional to k^0.

$$I = Ai_0 \left\{ \exp\left[\frac{\alpha_a nF}{RT} \left(E - E_{eq} \right) \right] - \exp\left[-\frac{\alpha_c nF}{RT} \left(E - E_{eq} \right) \right] \right\},$$

where $i_0 = FAk^0 C_O^{(1-\alpha)} C_R^{\alpha}$

Equation 4: Butler-Volmer.

Higher exchange current or current densities are indicative of high electron transfer rates, when the Faradaic redox reaction is carried out. An experimental way to determine the exchange current and the equilibrium potential is the Tafel plot. The Tafel plot can be represented as a dependence of the overpotential and the log of the current, log (i), or as the potential and the log of the current, log (i) (Figure 14).

The Tafel equation and Tafel plot are applicable at high overpotentials (> 0.05V). [18] In that case, the overpotential can then be considered logarithmically dependent on the current density, and the plots of overpotential versus log current density can be described by Tafel lines. Based on the Tafel plots, the OCP of the studied system and the exchange current can be determined. [19] We used the Tafel approach to study the redox potential of the S-POW itself and the influence of the additive amount on this parameter. The final goal was to find a correlation between the shifts in the polymer redox potential with the changes in the breakdown strength due to the presence of different amounts of the additive. The increase in breakdown strength of the S-POW due to the presence of an additive analyzed in Chapter 1 led to the interest in electrochemical studies of the additive as well as the additive/polymer complex. Solutions of the same concentrations of 2-NDPA in 9.7% (w/w) S-POW in chloroform were analyzed to determine if a correlation exists between the redox potential of the additive and or additive/polymer and the significant increase in breakdown strength of 1.0%, 0.2% and 0.5% additive compared to the control polymer. A 2.5% sample was added to the experiments for completeness. Solutions of the additive/polymer complexes (5 μL) were dropped on a glassy carbon electrode with geometrical surface area 0.03 cm^2 and air-dried. This electrode was then introduced in a three-electrode setup and explored as a working electrode. The reference electrode was quartz-sealed saturated Ag/AgCl, and Pt wire was utilized as counter electrode. 0.1M KOH with 0.1M KCl as indifferent electrolyte having an adjusted pH of 9.5 and 11.5 was used as the electrolyte for the electrochemical tests. Potentiostatic polarization experiments were performed by carrying out chronoamperometry measurements at different potentials starting from -1.0 to 1.0 V vs.

Ag/AgCl with a step of 0.1 V. The steady state current from each chronoamperometry measurement was used to create the Tafel plots. The polymer/additive composites examined are summarized in Table 3. The concentration of the additive when tested alone in solution (without polymer) was 1.0% (w/w) due to the impressive increase in breakdown strength at this concentration as discussed in Chapter 1.

Table 3. Mass fraction (w/w) of the additive in the chloroform polymer/additive solutions.

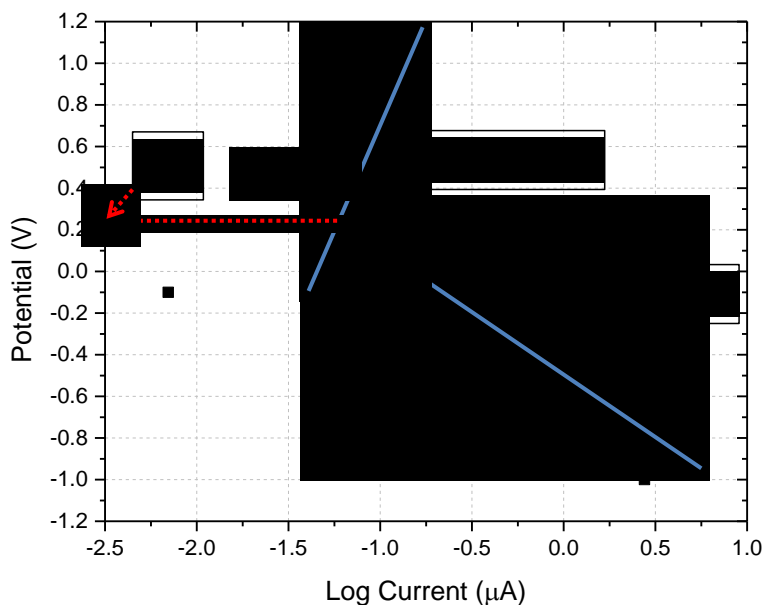| 2-NDPA Mass Fraction	Polymer Mass Fraction
0%	9.7% S-POW
0.10%	9.7% S-POW
0.20%	9.7% S-POW
0.50%	9.7% S-POW
1.00%	9.7% S-POW
2.50%	9.7% S-POW
5.00%	9.7% S-POW
1.00%	no S-POW

Figure 14. Tafel plot of 1.0% (w/w) 2-NDPA in S-POW at pH=9.5. The potential was measured vs. Ag/AgCl reference electrode.

Potential/current curves were obtained from the chronoamperometry measurements. The Tafel plot for 1.0% (w/w) 2-NDPA in S-POW at pH 9.5 was included in Figure 14 as an example. Based on that plot, the redox potentials of the polymer/additive mixtures were determined. The shape of the Tafel plots of the polymer/additive composites suggests i) non reversible electrochemical reaction with different number of electrons involved in the oxidation and the reduction processes; ii) small difference in the redox potentials of the polymer and the additive separately and therefore, only one redox potential can be seen on the plots; or iii) the polymer chemically interacts with the additive, producing one common polymer having the additive as a substitute and therefore only one redox potential can be detected. In the first case the mixed redox potential will be determined based on the redox potentials of the additive 2-NDPA and the polymer S-POW.

As can be seen from Table 4, the difference between the redox potentials of the additive and the polymer separately was large enough to obtain redox potentials associated with the oxidation/reduction of the additive and the polymer separately, influenced by the presence of the other composite in the mixture. Therefore we hypothesize that the polymer chemically interacts with the additive, forming one "new" polymer (Scheme 3). This "new" polymer then is oxidized/reduced during the electrochemical study.

Table 4. Redox potential of polymer/additive composites at pH 9.5 and pH 11.5.

2-NDPA Mass Fraction	Redox potential (V) at pH 9.5	Redox potential (V) at pH 11.5
0%	-0.025	-0.025
0.10%	0.1	0
0.20%	0.15	0
0.50%	0.175	0.05
1.00%	0.25	0.1
2.50%	0.4	0.25
5.00%	0.4	0.25
100%	-0.1 and -0.35	-0.1 and -0.35

Based on the fact that the nitro group has negative inductive and mesomeric effects, the election density at the o- and p- position in the benzene ring is decreased, and the substitution of the aromatic ring proceeds as meta-substitution. We assume that the phenyl substitute in the polymer structure was replaced by the additive, creating a covalent bond at the meta-position in the additive benzene ring.
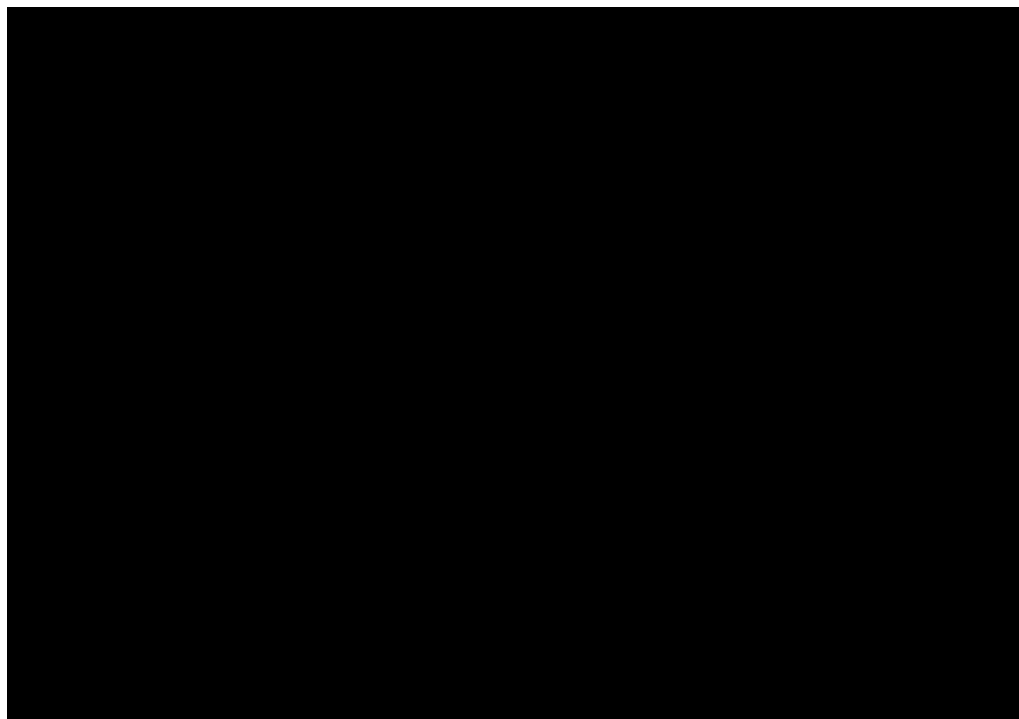
Scheme 3: Proposed mechanism for polymer/additive chemical interaction with subsequent electrochemical transformation.

To study the reduction reaction mechanism of this "new" polymer we performed potentiostatic polarization measurements at two pHs – 9.5 and 11.5. The redox potentials determined by this electrochemical test were plotted against the amount of the additive introduced to the original polymer at the two pHs (Figure 15). Obviously, there was a difference in the recorded redox potential at the two pHs indicating that protons were involved in the electrochemical reaction. The $\Delta E = E_{pH\ 9.5} - E_{pH\ 11.5}$ was approximately 120 mV for most of the polymer/additive composites suggesting that two protons are involved in the redox reaction and subsequently two electrons are also participating in it. Taking into account that NO_2 is an electron-withdrawing group we assume that particularly this group will be reduced/oxidized during the polarization.

A linear increase of the polymer redox potential with the increase in additive amount was found between 0.1 to 2.5% after which a saturation was observed indicating that the further increase of the additive mass fraction into the composite will not have an impact on the redox potential. The increase of the polymer redox potential will enhance its breakdown strength when we consider the polymer oxidation as the main mechanism for the breakdown. Therefore, we observed an increase of the polymer breakdown strength in presence of an additive until 1%, after which, at an additive mass fraction of 5% we saw again a drop in the strength likely due to significant morphological and chemical changes in the polymer structure.
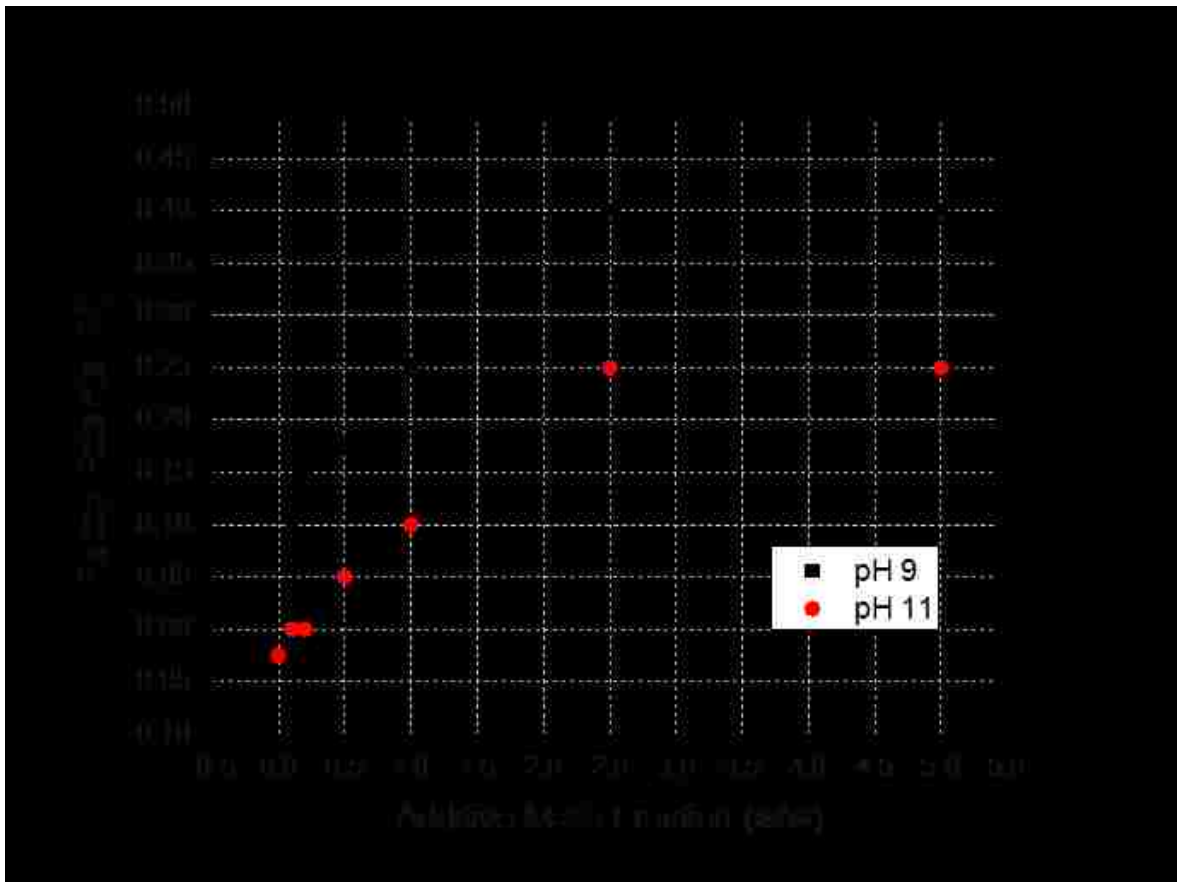
Figure 15. Dependence of the polymer/additive composite from the additive mass fraction.

The performed electrochemical study showed that there is a relationship between the composite redox potentials and the breakdown strength. The increased polymer potential led to enhanced polymer oxidative stability as it was expected.

Chapter 5

Evaluation and Characterization of Poly(PhNDI) and Poly(PhNDI)/Polynorbornene Copolymers

In order to be a feasible option for the automobile industry, high temperature thin film polymer dielectrics must meet specific criteria. The materials and methods of developing these dielectrics must be inexpensive and simple to meet demand. Solvent casting of films would be cost-prohibitive on a large scale, and these films commonly have many defects when compared to melt-extrusion films. In order to withstand extrusion, the polymer dielectrics must be thermally stable at high temperatures (~220 °C). In house extrusion was performed on S-POW using the extruder purchased from Dr. Collin® shown in Figure 16 but the resulting films were extremely brittle and unable to be successfully rolled into prototype capacitors without shorting during dielectric permittivity measurements. Figure 17 shows the comparison of a solvent cast S-POW film with an extruded film of relative thickness (~15 μm).

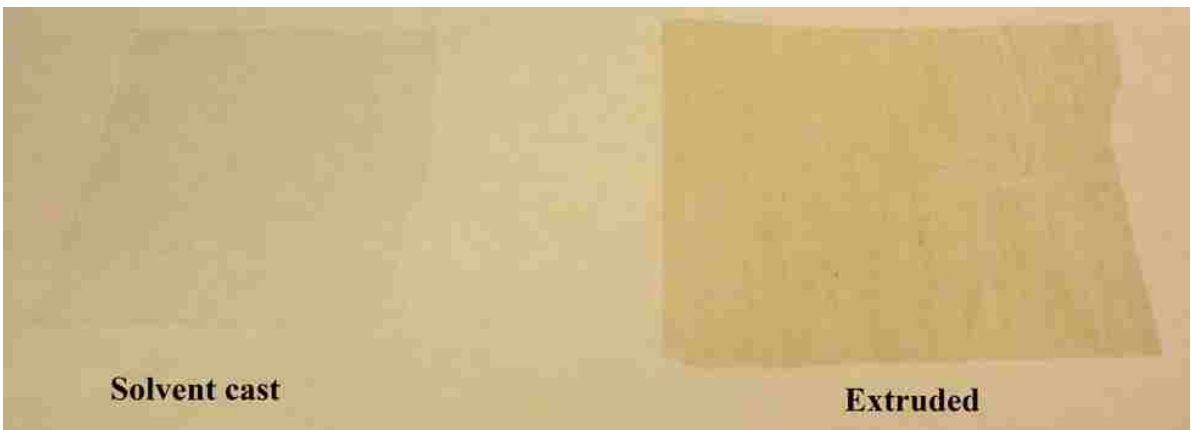**Figure 16.** Dr. Collin® extruder used for in-house extrusion of S-POW.

Figure 17. Solvent cast S-POW film produced via drawdown technique vs. extruded S-POW.

Upon visual inspection defects are not apparent in solvent cast S-POW films and a relatively transparent film is produced via the drawdown method despite no special care

being taken to prevent particulates from accumulating in the polymer films. A clean room would be necessary to completely limit this effect. Physical defects were initially observed in the extruded films as well as a color change when compared to solvent cast S-POW. As shown in Figure 18, TGA was performed to determine if decomposition of the polymer was occurring during extrusion; however, no significant T_d difference between extruded S-POW and solvent cast S-POW was observed. Additionally, dielectric permittivity measurements on the extruded S-POW film were not able to be performed due to the lack of quality of the film.
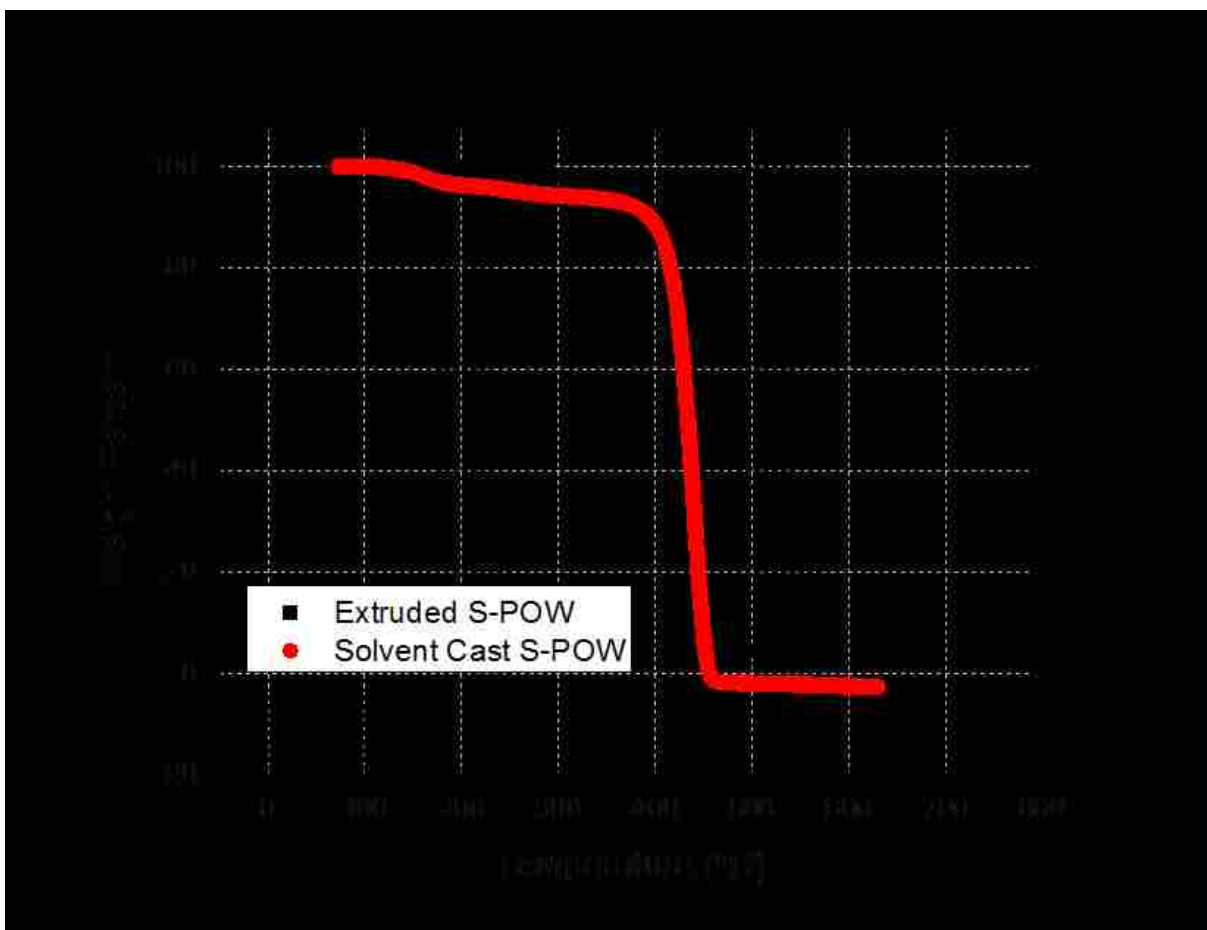

Figure 18. TGA curves of solvent cast S-POW vs. extruded S-POW.

Studies were performed evaluating the use of plasticizers in extruded polymer to increase flexibility. Plasticizers work by invading unused space of the polymer and increasing intermolecular distance resulting in swelling and increased free volume. [20] The plasticizer essentially acts as a lubricant within the polymer allowing more chain mobility and therefore better flexibility. Additionally, the plasticizers allow the polymer to remain more ductile at lower temperatures by reducing the T_g. However, in order for the plasticizers to be beneficial for the purpose of high temperature polymer dielectrics, a significant reduction of T_g is not acceptable.

Several plasticizers were screened including phthalates, terathanes, and trimellitates to improve the mechanical performance of the S-POW and optimize extrusion of the material. Plasticizers trioctyl trimellitate and 650, 1400, and 2900 terathanes were examined to improve the properties of the solvent cast S-POW films based on improved mechanical characteristics without a detrimental decrease in T_g (plasticizer characterization performed by Kirsten Cicotte). Ultimately 650 terathanes and trioctyl trimellitate were chosen for in-house extrusion studies and optimization. Several prototype capacitors were developed using the extruded polymer with the incorporation of these plasticizers. Photographs of one capacitor (10% (w/w) trioctyl trimellitate) are provided in Figures 19-20. Figure 21 shows that a concentration of 12% of both plasticizers resulted in severely diminished breakdown strengths in the extruded films while 10% (w/w) of the trioctyl trimellitate showed no adverse effect on the breakdown in S-POW.

Figure 19. 3 ft capacitor (prior to rolling) of extruded 10% (w/w) trioctyl trimellitate in S-POW.

Figure 20. 3 ft capacitor (post rolling) of extruded 10% (w/w) trioctyl trimellitate in S-POW.

While the introduction of plasticizers showed some improvement in mechanical properties, [21] incorporation of the plasticizers into the polymer proved difficult and posed a significant limitation in the optimization of in-house extrusion.
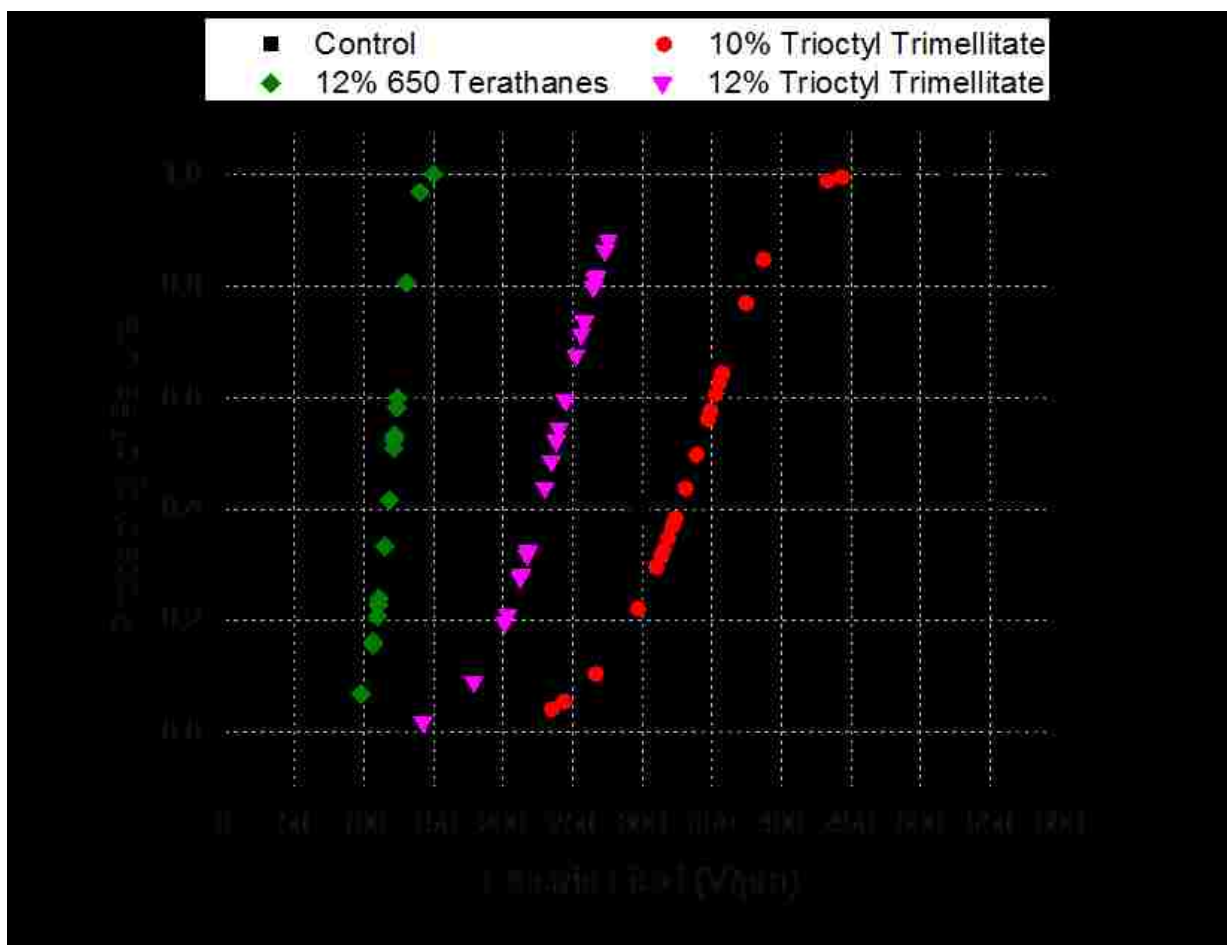
Figure 21. Breakdown results for plasticizers incorporated into extruded films vs. solvent cast S-POW (no plasticizer).

Recently Yoon *et al*. demonstrated a greater thermal stability and T_g of poly(N-phenyl norbornene 5,6-dicarboximide poly(NDI)), the carbon analog of poly(N-phenyl-7-oxanorbornene) poly(PhONDI) and it was found that the oxygen bridged polymer exhibited a lower degradation and glass transition temperature (Scheme 4). [22]
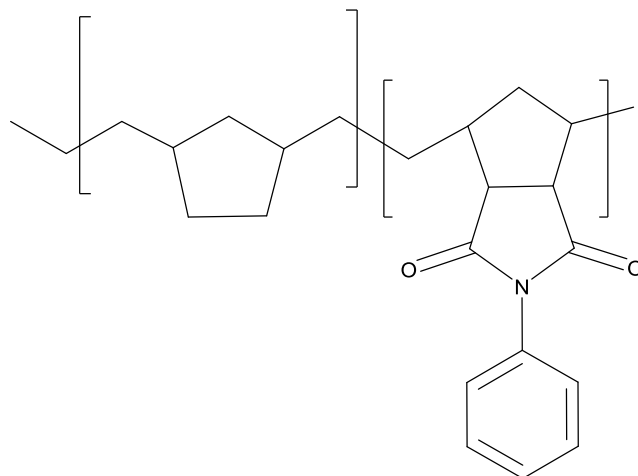
Scheme 4. Structure of poly(N-phenyl norbornene 5,6-dicarboximide poly(NDI)).

Therefore it was suspected that the oxygen bridge in the backbone of the poly(PhONDI) was causing degradation during the hydrogenation of the polymer into S-POW. Polymerizations of poly(PhNDI) were performed utilizing ROMP with Grubbs 3 ruthenium catalyst in chloroform at room temperature. Initially a 75:25 ratio of PhNDI to NBE copolymer was synthesized and hydrogenated in order to make a relevant comparison to S-POW in an attempt to confirm the dielectric properties of the new polymer. [23] A significant increase in breakdown strength of greater than 50 V/μm was observed for the PhNDI:NBE copolymer (Figure 22). Due to the higher thermal stability of the poly(PhNDI) and impressive improvement in energy density of the hydrogenated 75:25 PhNDI:NBE (carbon analog to S-POW) when compared to S-POW control, various ratios of PhNDI and NBE were synthesized and characterized to determine the effectiveness of poly(PhNDI) for use as a high temperature polymer dielectric.
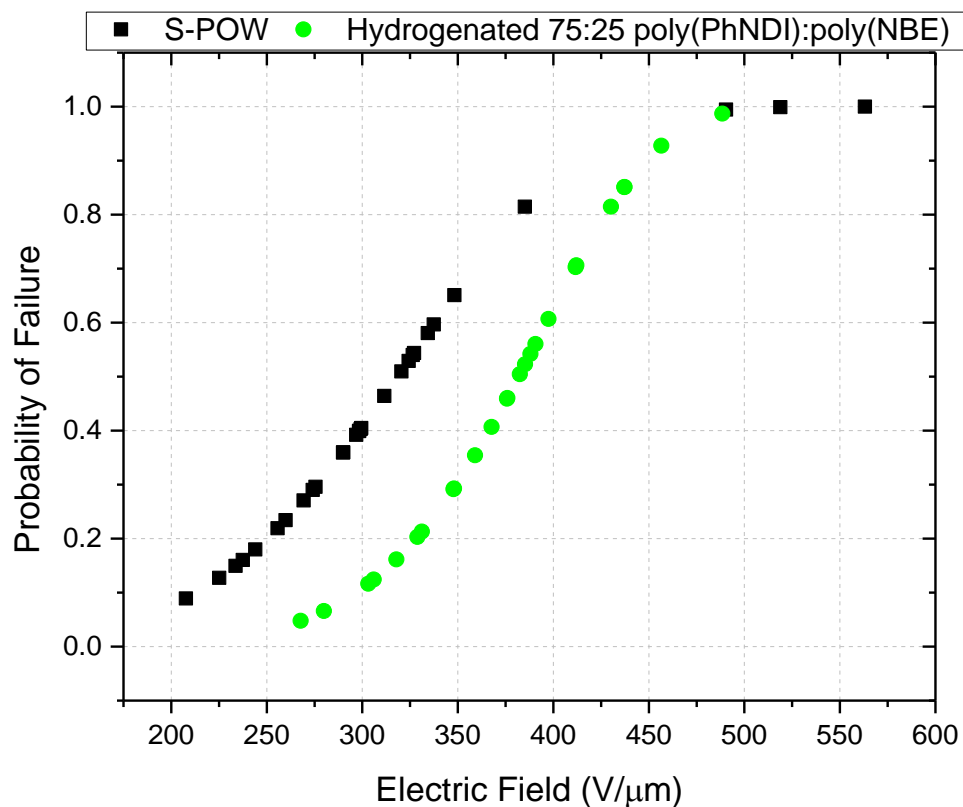
Figure 22. Breakdown comparison of S-POW vs. hydrogenated carbon analog.

The homopolymer of poly(PhNDI) was prepared in addition to three PhNDI:NBE copolymers as provided in Table 4.

Table 4. Stoichiometry of co-poly(PhNDI)-poly(NBE)

% NDI	% NBE
100	0
50	50

Figure 23 shows the DSC curves for the copolymers as well as the poly(PhNDI) homopolymer. The homopolymer provided the highest T_g (as expected); however, the films were brittle and difficult to work with. The 30 and 50 NDI demonstrated an unfavorable T_g of ~90 °C and ~125 °C while the 90 NDI matched the T_g of S-POW (175 °C).
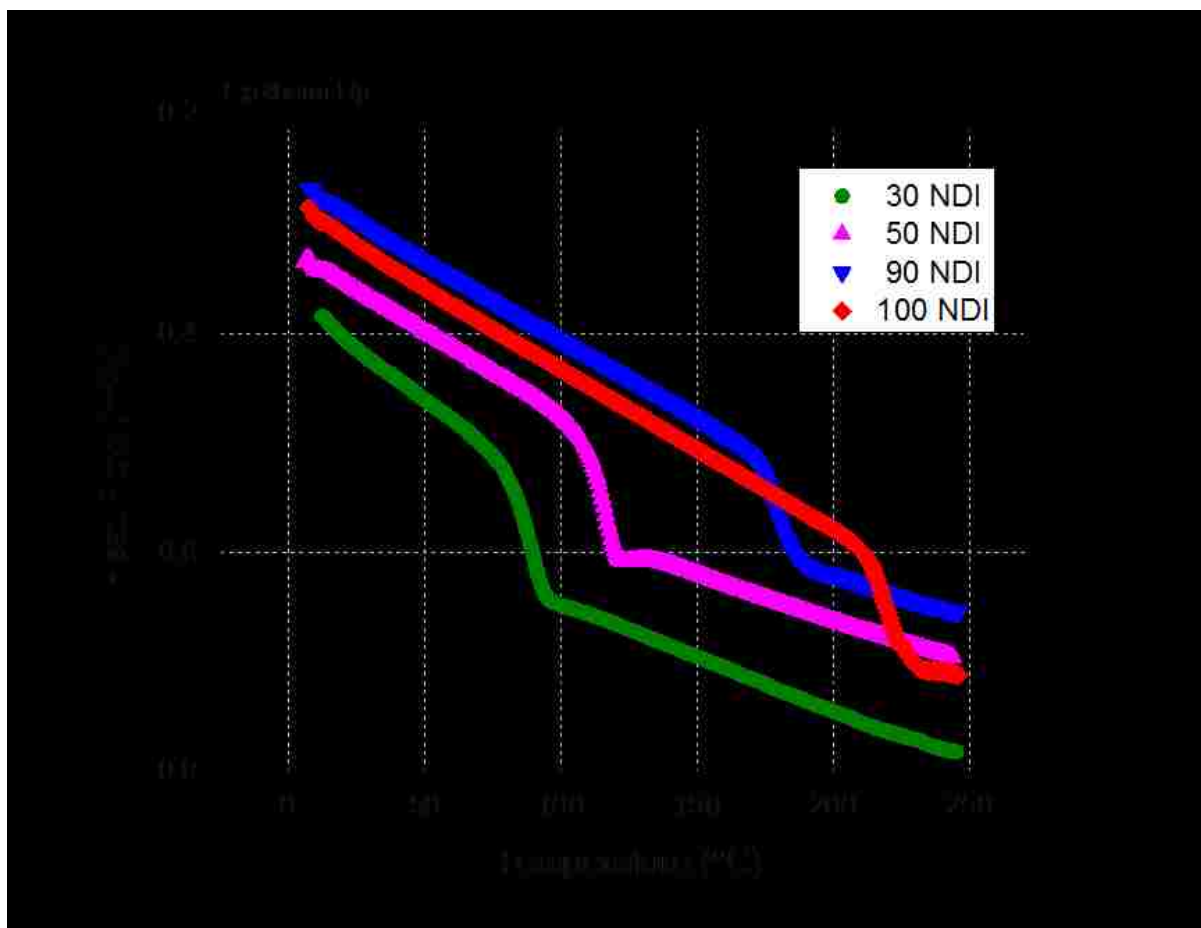

Figure 23. DSC curves for the homopolymer of poly(PhNDI) and three PhNDI:NBE copolymers.
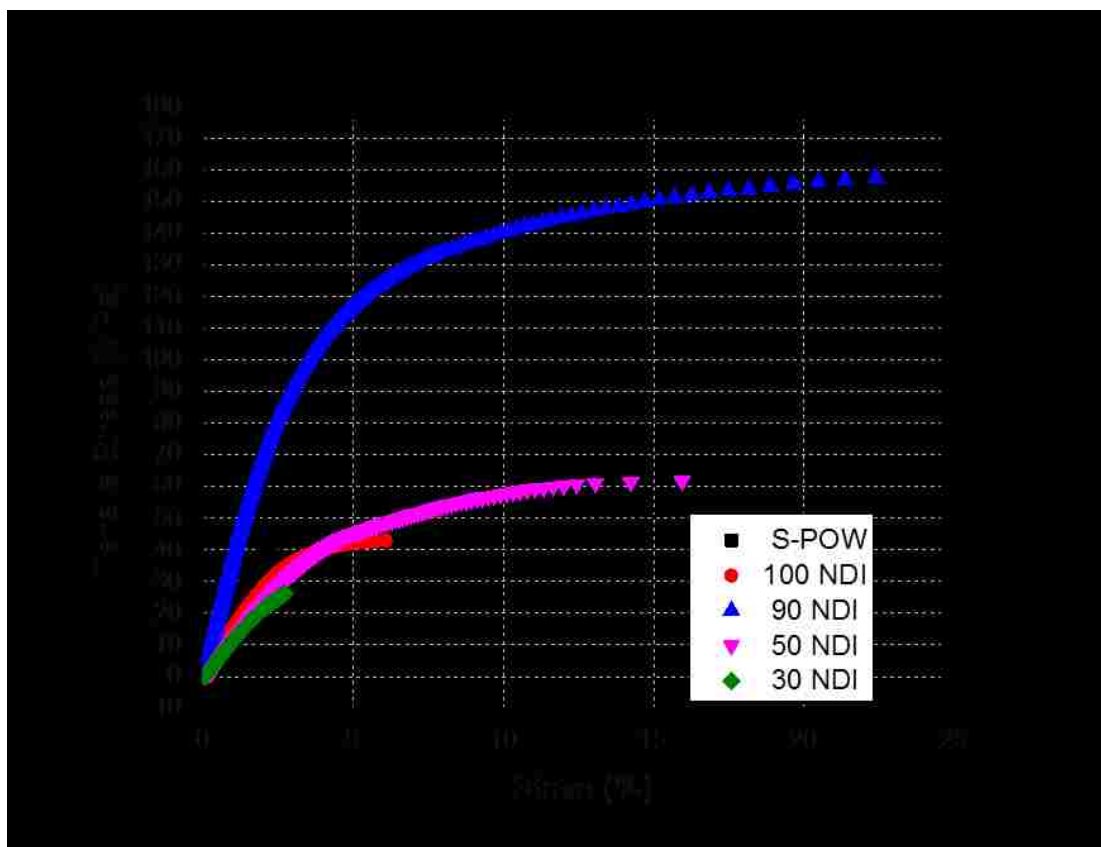
Figure 24. Stress-strain curves for the homopolymer of poly(PhNDI) and three PhNDI:NBE copolymers vs. S-POW.

The stress-strain curves of each of the polymer films are given in Figure 24. Increasing the imide monomer content in the copolymers showed an increase in the stress and the elongation at break. The imide homopolymer does not follow this trend and has values significantly lower than the 50 and 90 NDI copolymers. The 90 NDI displayed an impressive tenfold increase in elongation as well as a rise in tensile stress of 100 MPa when compared to S-POW. The overwhelming improvement in the mechanical properties should greatly improve processability of the dielectric polymer and permit melt extrusion into films allowing for the transition to industry.

Chapter 6

Conclusions and Future Work

The improvement of high temperature polymer dielectrics in HEV applications will significantly reduce the cost and volume while simultaneously increasing the operation temperatures of the DC bus capacitors. The low cost of our approach, calculated based on S-POW values ($< \$0.03/\mu F$), is a major incentive for the automotive industry. The high operation temperatures discussed here also allow for the removal of a cooling system in the HEV, further reducing cost and weight. With the introduction of the improved electrical properties of the S-POW copolymer with additive (2-NDPA) up to 1.0% (w/w) and the overwhelming mechanical characteristics of the 90 NDI copolymer, a transition of the lab scale process to industry should now be examined.

The work we have done with Electronic Concepts, Inc. (ECI) to develop a solvent casting technique as well as the extrusion technique developed at the Natick Soldier Center will allow more than 100 m of thin polymer films to be produced and used to fabricate next generation prototype capacitors. Inexpensive nanoparticle fillers will also be used to further increase dielectric breakdown strength and improve the relative permittivity of the high temperature polymer dielectrics in order to decrease capacitor volume and reach the 2020 VT goals.

References

1. Energy, U.S.D.o.E.E.E.a.R. *Vehicle Technologies Office*. Available from: https://www1.eere.energy.gov/vehiclesandfuels/.
2. Energy, U.S.D.o.E.E.E.R. *U.S. Drive*. Available from: https://www1.eere.energy.gov/vehiclesandfuels/about/partnerships/usdrive.html.
3. Ho, J.J., Richard, *Characterization of High Temperature Polymer Thin Films for Power Conditioning Capacitors*, A. Sensors and Electron Devices Directorate, Editor 2009.
4. You, Z., et al., *High dielectric performance of tactic polynorbornene derivatives synthesized by ring-opening metathesis polymerization.* Journal of Polymer Science Part A: Polymer Chemistry, 2013. **51**(6): p. 1292-1301.
5. Venkat, N., et al., *High temperature polymer film dielectrics for aerospace power conditioning capacitor applications.* Materials Science and Engineering: B, 2010. **168**(1–3): p. 16-21.
6. Anderson, R., *Select the right plastic film capacitor for your power electronic applications.* Ias '96 - Conference Record of the 1996 Ieee Industry Applications Conference, Thirty-First Ias Annual Meeting, Vols 1-4, 1996: p. 1327-1330.
7. Carter, M.A., *Film Capacitors for High Temperature Operation*.
8. Nash, J.L., *Biaxially oriented polypropylene film in power capacitors.* Polymer Engineering & Science, 1988. **28**(13): p. 862-870.
9. Winsor IV, P.L., Edward; Zafar, M.; Munshi, A.; Ibrahim, Iyad, *New Polymer Dielectric For High Energy Density Film Capacitors*.
10. Dirk, S.M., et al., *High temperature polynorbornene copolymer dielectric materials.* Abstracts of Papers of the American Chemical Society, 2009. **237**.
11. Lee, L.-B.W. and R.A. Register, *Hydrogenated Ring-Opened Polynorbornene: A Highly Crystalline Atactic Polymer.* Macromolecules, 2005. **38**(4): p. 1216-1222.
12. Mango, L.A. and R.W. Lenz, *Hydrogenation of Unsaturated Polymers with Diimide.* Makromolekulare Chemie-Macromolecular Chemistry and Physics, 1973. **163**(Jan): p. 13-36.
13. Denton, M.L.B., et al., *High Temperature Polymer Dielectrics from the ROMP reaction.* Journal of Applied Polymer Science, in prep.
14. Shawn M. Dirk, D.R.W., *Norbornylene-based polymer systems for dielectric applications*, 2008, Sandia Corporation.
15. Hunt, G.H., *Solid Dielectric Polyolefin Compositions Containing Voltage Stabilizers*, 1971.
16. Polymers, T.A.
17. Dirk, S.M., et al., *Thiol-ene coupling modifications of polynorbornene polymers for the synthesis of novel dielectric materials.* Polymer Preprints, 2010.
18. Bediako, D.K., et al., *Proton-Electron Transport and Transfer in Electrocatalytic Films. Application to a Cobalt-Based O-2-Evolution Catalyst.* Journal of the American Chemical Society, 2013. **135**(28): p. 10492-10502.
19. Cambridge, U.o. *The Tafel Plot*. 2013; Available from: http://www.doitpoms.ac.uk/tlplib/aqueous_corrosion/tafel_plot.php.
20. Sigma-Aldrich. Available from: http://www.sigmaaldrich.com/materials-science/material-science-products.html?TablePage=16371266.
21. Dirk, S.D., Michele.; Cicotte, Kirsten.; Johns, Kylen.; Belcher, Cami.; Fujimoto, Cy. *High Temperature Polymer Capacitor Dielectric Films*. 2013; Available from:

http://www4.eere.energy.gov/vehiclesandfuels/resources/merit-review/sites/default/files/ape009_fujimoto_2013_o.pdf.

22.   Yoon, K.-H., et al., *Synthesis and structure–property comparisons of hydrogenated poly(oxanorbornene-imide)s and poly(norbornene-imide)s prepared by ring-opening metathesis polymerization.* Journal of Polymer Science Part A: Polymer Chemistry, 2012. **50**(18): p. 3914-3921.

23.   Fujimoto, C.H., et al., *Synthesis and Characterization of Polynorbornene Derivatives for High Dielectric Applications.* Journal of Applied Polymer Science, in prep.